Mutational Mapping of Functional Residues in Tissue Factor: Identification of Factor VII Recognition Determinants in Both Structural Modules of the Predicted Cytokine Receptor Homology Domain†

Wolfram Ruf,* John R. Schullek, Martin J. Stone, and Thomas S. Edgington

Departments of Immunology and Molecular Biology, The Scripps Research Institute, 10666 North Torrey Pines Road, La Jolla, California 92037

Received September 22, 1993®

ABSTRACT: Alanine scanning mutagenesis of tissue factor, the initiating receptor and cofactor molecule for the coagulation pathways, was used to define residue side chains with functional contributions. Approximately half of the residues were exchanged, and several stretches of functional residues throughout the entire extracellular domain were identified which contributed to overall coagulant function. Mutants were further characterized with respect to their affinity for binding of ligand, providing evidence that identified functional sequence spans are involved in ligand interaction. The tissue factor extracellular domain is suggested to adopt the folding pattern of the cytokine receptor homology unit, which is typically composed of two seven-β-strand modules. Evaluation of the mutational analysis within this structural context suggests that functionally important residues are spatially proximate and clustered at the boundary of the predicted β-strand modules. Residues contributing to ligand binding by tissue factor were identified in positions corresponding to ligand interactive residues in the growth hormone receptor and contact residues of other cytokine receptors, consistent with a conserved structural region for ligand interaction throughout the cytokine receptor family.

Cellular initiation of the coagulation pathways *in vivo* is mediated by the cell surface receptor tissue factor (TF)[1] (Davie et al., 1991; Edgington et al., 1991). TF serves as the receptor for coagulation factor VIIa (VIIa) and the zymogen precursor factor VII (VII) which is rapidly activated in the TF·VII complex by selected proteases, including factors Xa or IXa and the TF·VIIa complex (Rao & Rapaport, 1988; Nakagaki et al., 1991). TF is a macromolecular catalytic cofactor for VIIa by changing the catalytic efficiency of the bound protease, as evaluated with small peptide analogue pseudosubstrates (Ruf et al., 1991c; Lawson et al., 1992). Independent of the enhancement of catalytic function determined with small peptidyl substrates, TF supports the cleavage of protein substrates, and this function has been assigned to specific residues in the sequence 156–174 by scanning alanine mutagenesis (Ruf et al., 1992a,b). The residues in TF which mediate the assembly of the TF·VIIa complex have not been identified. However, antibody mapping (Ruf et al., 1991b; Ruf & Edgington, 1991a), chemical cross-linking of receptor and ligand (Ruf & Edgington, 1991b), functional characterization of proteolytic fragments (O'Brien et al., 1993), and structurally disruptive mutational analysis (Rehemtulla et al., 1991) suggest that there is not a single linear sequence span that mediates the interaction with the ligand protease VIIa and that residues distributed through the extracellular domain of TF contribute to ligand binding. In this study, we provide a mutational mapping to search for functional residues of TF. On the basis of Ala exchange mutagenesis, we propose an overall topographical assignment of functional and nonfunctional regions in TF. We further identify residues which are required for binding of VIIa providing an initial localization of key residues which may form the ligand interface in TF.

EXPERIMENTAL PROCEDURES

Mutagenesis and Expression of TF. Mutants of TF were generated by oligonucleotide-directed mutagenesis using the TF coding sequence cloned into the expression vector CDM8 as the template DNA, as previously described in detail (Ruf et al., 1993). For functional analysis, the mutants were expressed by transiently transfecting Chinese hamster ovary (CHO) cells with the expression plasmid. Transfected cells were harvested 48 h after transfection and stored in appropriate aliquots at −70 °C for functional analysis and immunoassay.

For circular dichroism (CD) and ^{1}H nuclear magnetic resonance (NMR) spectroscopy, the mutants and wild-type TF were expressed as soluble truncation mutants (residues 1–218) in *Saccharomyces cerevisiae*. The coding sequence for residues 1–218 was recovered from the mammalian cell expression plasmid employing the polymerase chain reaction, and the same step was used to change the triplet encoding residue 219 to a termination codon. The amplified product was subcloned into the *Stu*I site of the *Escherichia coli*/*S. cerevisiae* shuttle vector pMFα8 (Miyajima et al., 1985) by *in vivo* recombination (Jones & Howard, 1991). Yeast strain GRY697 (*MAT*α, *trp1-1*Δ, *ura3-52*) was transformed with the expression plasmid, and transformed cells were selected on Trp deficient culture plates. TF was purified from the yeast culture broth by immunoaffinity chromatography (Ruf et al., 1991c) followed by ion exchange chromatography on MonoQ (Ruf et al., 1992c).

Immunoassay. The concentration of mutant or control wild-type TF in the transfected CHO cells was determined by immunoassay, as described in detail (Ruf et al., 1992a, 1993). Briefly, a defined aliquot of pelleted cells was lysed in 6 mM CHAPS (3-[(3-cholamidopropyl)dimethylammonio]-1-propanesulfonate), and the cell lysate was serially diluted for

† This work was supported by National Institutes of Health Grant PO1-HL-16411 from the National Heart, Lung and Blood Institute.
® Abstract published in *Advance ACS Abstracts,* February 1, 1994.
[1] Abbreviations: tissue factor, TF; factor VII/VIIa, VII/VIIa; Chinese hamster ovary cells, CHO cells.

0006-2960/94/0433-1565$04.50/0

immunoassay based on two monoclonal antibodies to nonoverlapping epitopes. Typically two or three of the serial dilutions gave concordant results in TF concentration, and the mean of these data points derived from the linear part of the calibration range was calculated. Assays were repeated at least three times for each mutant, and the presented data are mean values calculated from determinations on different occasions. In cases where specific antibody epitopes were affected by the Ala exchange (see below), the immunoassay was based on different pairs of monoclonal antibodies which did not reveal decreased binding of the respective mutant.

Evaluation of Overall Function by Coagulation Assay. Mutants were analyzed for function by a one-stage coagulation assay. Assay procedure and precision for the coagulation assay have been described in detail (Ruf et al., 1992a). Briefly, an aliquot of pelleted cells was lysed with 15 mM octyl β-D-glucopyranoside in 10 mM Hepes, 140 mM NaCl, pH 7.4, by vigorous vortexing for 1 min followed by a 15-min incubation at 37 °C. Serial dilutions were analyzed and coagulant activity was derived from double logarithmic calibration curves of clotting times versus serial dilutions of wild-type TF. Typically, two dilutions from the linear portion of the calibration range were used to calculate the coagulant activity, and assays were repeated on three separate occasions. Coagulant activity was normalized on the basis of the antigen concentration to yield the specific activities for mutant and wild-type TF. Loss of specific activity was calculated relative to wild-type TF which was transfected and analyzed in parallel. The data represented are based on the mean values from the replicate determinations.

Determination of k_{Dapp}. To analyze the importance of specific residues for binding of VIIa, a linked chromogenic assay with purified recombinant VIIa (Novo Nordisk) and factor X which was purified as previously described (Ruf et al., 1991c) was used. Wild-type or mutant TF (1–6 pM) from octyl glucopyranoside cell lysate prepared as described above was assembled with recombinant VIIa (0.5 pM to 15 nM) at 5 mM Ca^{2+} for 10 min at 37 °C. In preliminary experiments, maximum functional activity of the TF·VIIa complex was obtained within 3 min, suggesting that equilibrium within the 10-min preincubation was approximated. Formed TF·VIIa complexes were quantified with substrate factor X added at 100 nM for a fixed time at 37 °C, followed by quenching of the reaction with 50 mM EDTA (Ruf et al., 1992a,b). The rate of chromogenic substrate Spectrozyme FXa hydrolysis by the formed factor Xa was determined in a 96-well multichannel ELISA reader in the kinetic mode at ambient temperature (Molecular Devices, Menlo Park, CA). The rate of substrate hydrolysis was converted to formed TF·VIIa complexes using the hydrolysis rate at saturation and the concentration of TF determined by immunoassay. Enzfitter (Elsevier Biosoft) programs were employed to calculate the K_{Dapp} from the experimentally determined bound VIIa and free VIIa, which was obtained by subtracting bound VIIa from the initial VIIa concentration. The calculated K_{Dapp} values for mutant TFs represent the mean values from at least three independent determinations with coefficients of variation <25%. The K_{Dapp} was not influenced by increasing or decreasing the time period for the activation of factor X by 2-fold, suggesting that the equilibrium of the TF·VIIa complex does not change slowly following the addition of substrate. Further, increasing or decreasing the factor X concentration 4-fold did not result in detectable changes of the K_{Dapp}, indicating that substrate was not limiting and that the substrate factor X does not influence the functional K_{Dapp} determination under these assay conditions, consistent with other studies (Krishnaswamy, 1992).

Western-Blot Analysis and Assessment of Antibody Reactivity. Mutant and wild-type proteins expressed in mammalian cells were assessed for post-translational modification and intracellular degradation by Western-blot analysis of cell lysate. Typically, a pellet of 1×10^6 CHO cells was resuspended in SDS-sample buffer and separated by polyacrylamide gel electrophoresis followed by electrophoretic transfer to nitrocellulose. A polyclonal antibody to human TF was used to provide immunochemical detection of intact as well as degraded TF in the cell lysate using standard alkaline phosphatase technology, as previously described (Ruf et al., 1991b). For specific mutants (see Results), this analysis revealed evidence for increased intracellular degradation and for changes in the glycosylation pattern relative to wild-type TF. This has previously been observed upon structurally disruptive mutations in TF (Rehemtulla et al., 1991), and these criteria have been adopted here as indications of misfolded mutant protein. As additional screening for global conformational alteration, the reactivity of mutants with monoclonal antibodies was analyzed by inhibition of function. Briefly, mutant or wild-type TF in an octyl glucopyranoside cell lysate were incubated for 30 min with each of the previously characterized inhibitory and conformation-dependent monoclonal antibodies (30 μg/mL) to three nonoverlapping epitopes on TF (Ruf et al., 1991b), followed by quantitation of residual coagulant activity in comparison to a noninhibited sample. Reduction in antibody inhibition by 10% compared to wild-type TF was considered evidence for loss of structure necessary for antibody reactivity.

Structural Analysis of TF Mutants. The indirect approaches employed to evaluate potential structural alterations were complemented by direct physicochemical analysis of selected dysfunctional mutants in the amino-terminal and carboxyl-terminal halves of the TF extracellular domain. The isolated extracellular domains of wild-type and mutant TFs were analyzed by CD and 600-MHz ^{1}H-NMR spectroscopy. CD spectra were generated on an Aviv 61DS spectropolarimeter at a protein concentration of ≈20 μM in 50 mM NaCl, 2.5 mM phosphate, 50 μM EDTA, pH 7.0. ^{1}H-NMR spectra were recorded on a Bruker AMX600 spectrometer with samples (50–200 μM) in D_2O, 50 mM NaCl, 2.5 mM phosphate, 50 μM EDTA, pH 7.0. The residual H_2O resonance was suppressed by preirradiation.

RESULTS

Mapping of Regions Critical for TF Function. We used scanning Ala mutagenesis to identify residue side chains which are important for function of TF. We randomly chose residues for exchange throughout the TF extracellular domain sequence, but we excluded the 24 Gly, Pro, and Cys residues from the analysis presented here, because of the frequently observed importance of Gly and Pro residues for the peptide backbone conformation and resulting structural alterations upon Ala replacement. From the remaining 188 non-Ala residues of the TF extracellular domain, we exchanged 104 with Ala, including 12 of the 24 aromatic residues and 40 of the 54 charged residues. Initially, multiple substitutions were employed to expedite the search. These were followed in regions yielding significant loss of function by single Ala substitutions.

Mutants which were expressed in mammalian CHO cells as full length transmembrane proteins were analyzed by coagulation assay as an approximation for overall biological

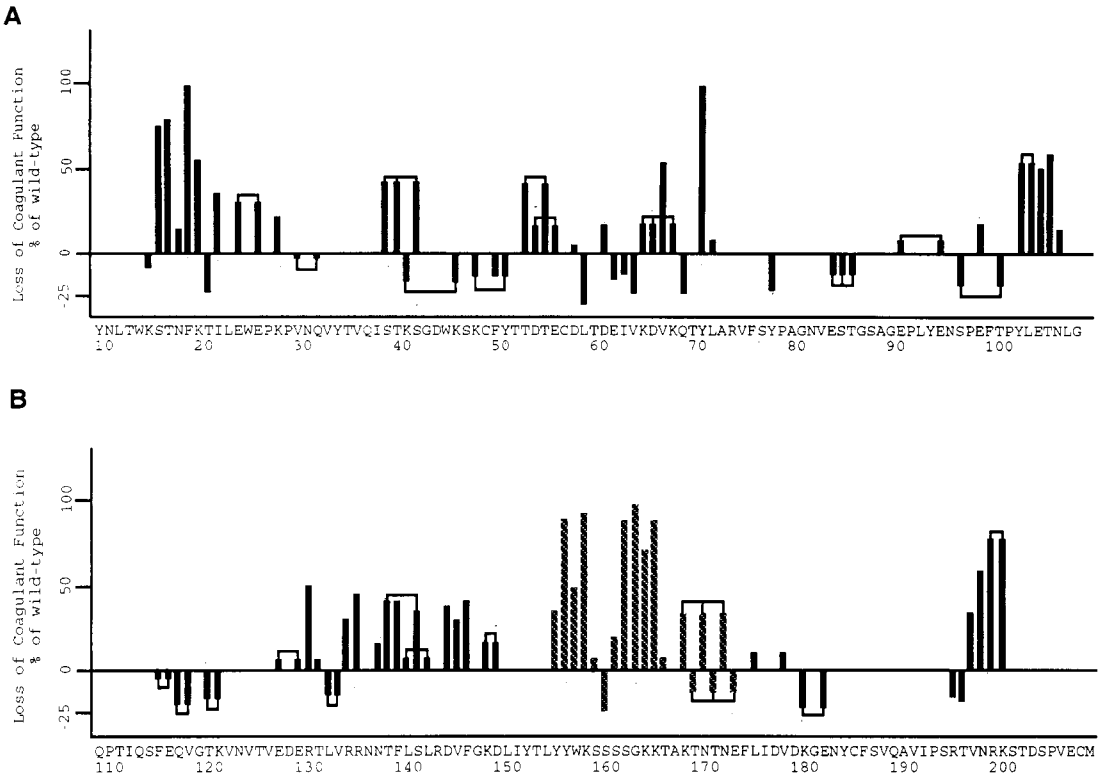

FIGURE 1: Functional characterization of site-directed Ala replacements for residues in TF. Mutants in the sequence 10–109 (panel A) and 110–210 (panel B) are identified by the replaced residue in single-letter amino acid code. Linked bars indicate multiple Ala substitutions in a single mutant. The bars represent the reduction in specific coagulant activity expressed as percent of wild-type activity (100% – (specific activity mutant/specific activity wild-type)%). The hatched bars represent previously reported data from the scanning Ala mutagenesis of the sequence 156–174 (Ruf et al. 1992a,b).

function. The functional activity was normalized on the basis of the mutant concentration established by immunoassay. The loss in specific functional activity relative to wild-type TF which was transfected and analyzed in parallel is illustrated in Figure 1. For comparison, Figure 1 also shows the results from the scanning Ala mutagenesis of the 156–174 region (hatched bars), which has previously been analyzed in detail and shown to specifically support the activation of macromolecular substrate (Ruf et al. 1992a,b). Besides this prominent region of functionally important residues, loss of function appeared to be associated with mutations of various residues in the sequences 16–26, 103–106, 129–147, and 197–201. A 30–98% loss of specific function was observed for the Ala mutants replacing residues Ser^{16}, Thr^{17}, Phe^{19}, Lys^{20}, Ile^{22}, and Glu^{24}/Glu^{26}. Approximately 50% loss of function followed the replacement of Tyr^{103}/Leu^{104}, Glu^{105}, or Thr^{106}. Reductions of 30–50% in function were observed upon exchange of Arg^{131}, Arg^{135}, Arg^{136}, Thr^{139}/Ser^{142}, Phe^{140}, Asp^{145}, Val^{146}, or Phe^{147}. Replacement of Val^{198}, Asn^{199}, or Arg^{200}/Lys^{201} reduced function 30–80%.

Other mutants which lost overall function appeared to be not embedded in a longer linear stretch of functionally important residues. In particular, a triple mutant incorporating the Ser^{39}, Thr^{40}, and Ser^{42} exchange to Ala exhibited a 43% loss of function, and a double mutant replacing Thr^{53} and Thr^{55} lost function by 40%, suggesting that at least one of the replaced residues in each mutant contributed to function. Single-residue exchanges of Val^{67} and Tyr^{71} decreased function by 53% and 98%, respectively. The mutational analysis thus identified clusters in which more than 50% of the residues were required for function as well as functionally important residues which appear to be isolated in the context of linear sequence. Mutational exchange of the other residues shown in Figure 1 failed to diminish function by more than 25%. The negative results are also considered relevant, since some of the regions, e.g., residue sequence 116–121, were systematically mutated and none of the mutants showed loss of function.

Structural Integrity of Dysfunctional Mutants. In order to investigate whether reductions in function resulted from global structural alterations, the structural integrity of mutants was assessed. For all mutants the indirect criteria of efficient cellular expression as well as glycosylation by the mammalian cells in a pattern typical for the control wild-type TF were adopted as evidence for the highly discriminating cellular recognition and processing of a properly folded protein. The severely dysfunctional mutant $Phe^{19} \rightarrow$ Ala (Figure 1) was expressed at low levels and, on the basis of Western-blot analysis of cell lysate, exhibited significant fragmentation, suggesting structural alterations leading to increased intracellular degradation. The $Tyr^{71} \rightarrow$ Ala mutant was also poorly expressed, but appeared to be properly glycosylated without evidence of significant intracellular degradation, implying that the global folding of this mutant was unaltered. All other mutants were expressed at levels and with apparent glycosylation patterns comparable to those of control wild-type TF. Reactivity of the mutants with characterized inhibitory monoclonal antibodies to three nonoverlapping and conformation-dependent epitopes in both structural modules was analyzed as additional evidence for properly folded mutant protein. These monoclonal antibodies to both structural modules were reactive with all mutants except for those where sequence spans were mutated which have previously been assigned to the antibody epitope (Ruf et al., 1991b). On the basis of these independent criteria, all but the Phe^{19} mutant adopted proper global folding. The diminished function can therefore be attributed either to subtle local conformational alterations in an interactive site or to the removal of amino acid side chains directly contributing to function.

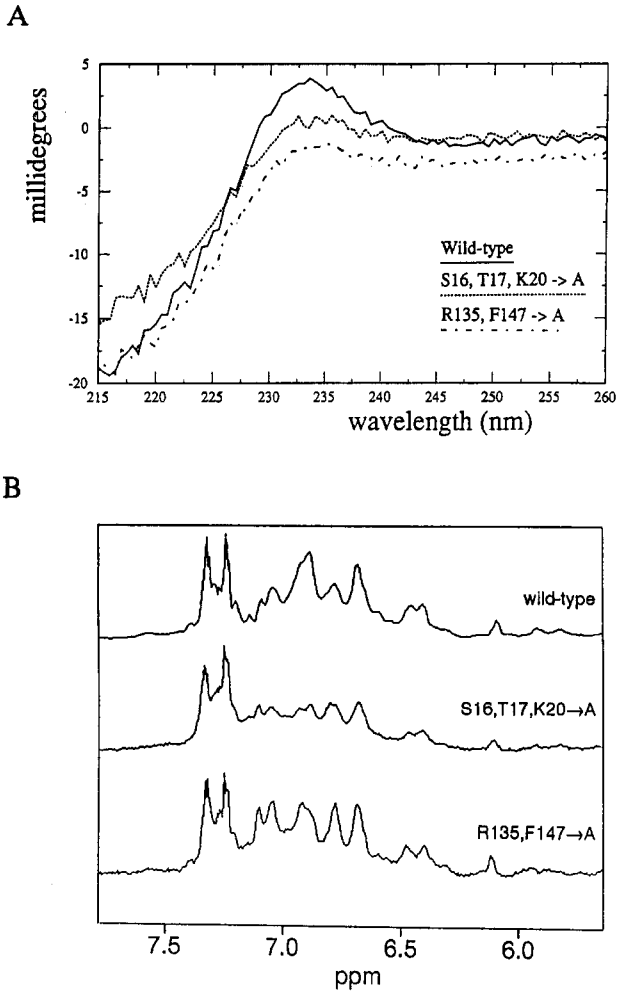

FIGURE 2: Circular dichroism spectra (panel A) and aromatic regions of the 600-MHz ^{1}H-NMR spectra (panel B) of selected TF mutants. The isolated and soluble TF extracellular domains (residues 1–218) of wild-type and mutant TF were expressed in yeast for structural analysis. Spectra were obtained in 50 mM NaCl, 2.5 mM phosphate, 50 μM EDTA, pH 7.0 buffer, either in H_2O for circular dichroism or in D_2O for NMR analysis.

Structural integrity of selected dysfunctional mutants was further directly evaluated by CD and ^{1}H-NMR spectroscopy. We chose to analyze mutants with multiple amino acid substitutions and hence a greater (>97%) loss of specific function in order to increase the probability for identification of structural alterations. We analyzed the Ser^{17} → Ala/Thr^{18} → Ala/Lys^{20} → Ala and the Arg^{135} → Ala/Phe^{147} → Ala mutants as prototypes for the functionally relevant regions 16–26 and 129–147, respectively. The CD spectra (Figure 2A) of these mutants exhibited typical 233-nm maxima as found in wild-type TF, although the intensity of the signal for the mutant Arg^{135} → Ala/Phe^{147} → Ala was somewhat decreased, presumably due to the removal of the aromatic side chain in this mutant. We further employed the extreme sensitivity of NMR chemical shifts (Ösapay & Case, 1991) as an additional and reliable probe of structural alterations. The ^{1}H-NMR spectra of the multiple mutants all exhibited features typical of wild-type TF (aromatic regions shown in Figure 2B). In particular, well-resolved peaks in the 6.9–6.5 ppm region, presumably shifted upfield by ring currents in the hydrophobic core, are unchanged in all mutants. Slight spectral changes in the 6.7–7.2 ppm region may be attributed to removal of aromatic residue side chains or possibly local conformational alterations, but these spectra are inconsistent with a mutant protein with significantly altered overall structure. These analyses are thus consistent with the indirect criteria used to assess the conformational integrity of the mutants.

Importance of TF Residues for Binding of VIIa. In order to assess the effect of the mutations on binding of ligand VIIa, we determined an apparent dissociation constant (K_{Dapp}) in a functional assay applicable to the necessity for replicate analyses of the large number of generated mutants. We established assay conditions to generate a reproducible estimate for a functional K_{Dapp}. Considering the large differences in reported K_D values for VIIa binding to TF and the recently reported tight binding with a K_D of 7 pM (Waxman et al., 1992), we evaluated the possibility that some of the higher K_D values reported in the literature represent upper limits due to a high receptor concentration in the assay. The functional K_{Dapp} was observed to progressively decrease when the TF concentration in the assay was reduced. At 1–6 pM TF, a K_{Dapp} for wild-type TF of 4.1 ± 1.0 pM (mean ± standard deviation, n = 16) was determined, and no further decrease was observed when the TF concentration was lowered to 0.5 pM. The K_{Dapp} determined by the functional assay is thus consistent with the lower limit described under equilibrium conditions (Waxman et al., 1992). Further, there is no evidence for an influence of substrate factor X on the K_{Dapp} determination, as demonstrated by the analysis of mutants in the 156–174 region. If the K_{Dapp} would depend on factor X hydrolysis, one would expect changes in the K_{Dapp} of mutants which are defective in providing full support for activation of macromolecular substrate, as in the case of the Tyr^{157} → Ala and Lys^{165} → Ala/Lys^{166} → Ala mutants. However, the K_{Dapp} determined for these mutants here was found to be indistinguishable from that of wild-type TF (Figure 3). This is consistent with extensive previous analysis indicating normal binding of VIIa to these mutants (Ruf et al. 1992a,b) and argues that the K_{Dapp} assay is not dependent on the macromolecular substrate used to quantify the formed TF·VIIa complexes under the conditions employed here.

The analyses of the site-directed mutants identified residues which were important for binding of VIIa. Several key residues were clustered in the 16–26 sequence. The Lys^{20} → Ala, Ile^{22} → Ala, or the Glu^{24} → Ala/Glu^{26} → Ala mutants exhibited 35-, 12-, or 3.8-fold increases in the K_{Dapp} compared to wild-type TF (Figure 3). The Asp^{58} → Ala exchange increased the K_{Dapp} 41-fold. Although the single Tyr^{71} → Ala exchange could not be adequately evaluated due to low expression levels, the K_{Dapp} was increased 2.1-fold for the Val^{64} → Ala/Tyr^{71} → Ala double mutant. A 2.2-fold increase in K_{Dapp} was observed for the Glu^{91} → Ala/Glu^{95} → Ala mutant. Arg^{135} or Phe^{140} substitutions by Ala increased the K_{Dapp} 7.4- and 18-fold, respectively, whereas the Arg^{196} replacement resulted in a 3.1-fold-increased K_{Dapp}. All other mutants shown in Figure 3 had <2-fold changes in the K_{Dapp} compared to wild-type TF. Some of the subtle increases in K_{Dapp} are nevertheless considered significant. In particular, the Leu^{133} → Ala/Val^{134} → Ala and the Glu^{128} → Ala/Glu^{130} → Ala double mutants are localized within the functionally important region 129–147 and demonstrated a 1.9- or 1.7-fold-increased K_{Dapp}, respectively. In summary, analyses of the apparent dissociation constants identified key residues throughout the TF extracellular domain sequence which contribute to the binding of VIIa.

Residues which contribute to coagulant as well as VIIa binding function appear to be colocalized, in particular in the sequences 16–26 and 129–147. However, single residues with significant contributions to binding of VIIa frequently ex-

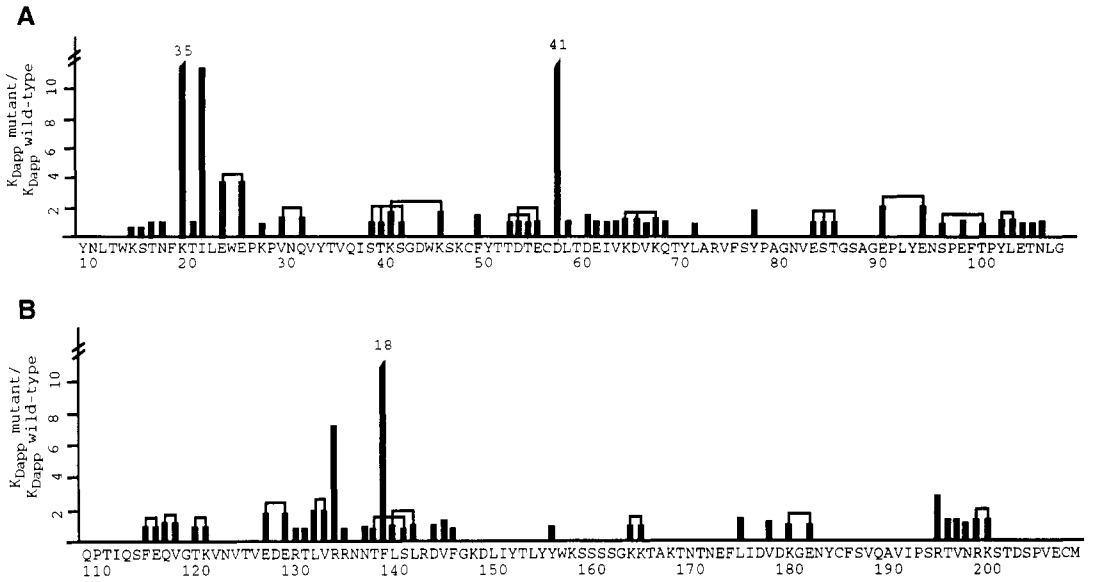

FIGURE 3: Functional K_{Dapp} for site-directed Ala mutants in TF. Mutants in the sequence 10–109 (panel A) and 110–210 (panel B) are identified by the replaced residue in single letter amino acid code. Linked bars indicate multiple Ala substitutions in a single mutant. The change in apparent K_D (ratio of K_D mutant to K_D wild-type) is shown. Data presented are mean values from at least three determinations at different occasions with coefficients of variation <25%.

hibited only minor decreases of overall coagulant function. A rationalization for this observation may be provided by the fact that the VII/VIIa concentration in the clotting assay is well in excess of 1 nM and thus close to 10^3-fold above the functional K_{Dapp}. Even a 41-fold-increased K_{Dapp}, as for the $Asp^{58} \rightarrow$ Ala mutant, could be without a significant effect on the coagulant activity, because the concentration of VII/VIIa would still considerably exceed the K_{Dapp} and saturation of the added TF could be achieved. To address this hypothesis experimentally, the activity of selected mutants was analyzed in VII/VIIa-depleted plasma supplemented with 1% (~0.1 nM VII/VIIa) or 10% (~1 nM VII/VIIa) normal human plasma. Compared to the activity of wild-type TF, the specific activities of the $Lys^{20} \rightarrow$ Ala, $Asp^{58} \rightarrow$ Ala, or $Phe^{140} \rightarrow$ Ala mutants were now decreased to 8%, 25%, or 15% at 10% normal plasma and to 0.9%, 2%, or 0.2% at 1% normal plasma, respectively. These data are consistent with the hypothesis that the only slightly reduced coagulant activity of mutants which have significant loss of binding function is a consequence of the relatively high plasma concentration of VII/VIIa compared to the K_{Dapp}.

DISCUSSION

This study was designed to develop an overall assignment of functional and nonfunctional regions in the TF extracellular domain using the side chain capping approach of site-directed Ala replacement mutagenesis. In addition to the previously characterized functionally important residues in the sequence 156–174 (Roy et al., 1991; Ruf et al. 1992a,b) which contribute selectively to the activation of macromolecular substrate, we here identify several residues which were required for full overall functional activity of TF. These residues were found in discrete and discontinuous sequence spans throughout the TF extracellular domain (Figure 1). Several of the residues suggested to be involved in overall function also demonstrated loss of affinity for VIIa, based on a functional K_{Dapp} estimate for the Ala replacement mutants. Key residues which are characterized by loss of both coagulant and VIIa binding function were thus identified throughout the sequence, in particular within sequence spans 16–26 and 129–147. This analysis thus provides an overall assignment of key residues and regions presumed to form the ligand binding site in TF.

The presented mutational mapping of functional residues in TF is consistent with previous analyses to delineate, though less precisely, the ligand binding structures in TF. Proteolytic amino-terminal truncation of TF at residue 35 reduced the affinity for binding of ligand (O'Brien et al., 1993) in agreement with the assignment of the sequence 16–26 as a major site for binding of VIIa. Asp^{58} is localized within the recognition sequence of anti-peptide antibodies against residues 40–71. These antibodies and monoclonal antibodies to the carboxyl-terminal aspect of the sequence 1–83 both strongly inhibit binding of VIIa to TF (Ruf et al., 1991b), consistent with a role of Asp^{58} as a contact residue for VIIa. The spatial proximity of residues 44–84 to ligand is further supported by chemical cross-linking to VIIa after complex formation (Ruf & Edgington, 1991b). Antibodies to residues 94–121 of TF inhibit binding of ligand (Ruf et al., 1991b), supporting some contribution of Glu^{91} and/or Glu^{95} or the sequence 103–106 to ligand interaction. The ligand binding residues within the 129–147 sequence are contained within a site in the carboxyl-terminal half of the TF extracellular domain which has been found to be spatially close to VIIa by chemical cross-linking (Ruf & Edgington, 1991b). The mutational analysis and independent experimental approaches thus concordantly implicate specific sequence spans in the binding of ligand VIIa, which lends support to the overall assignment of ligand binding structure suggested here.

A large number of mutants with loss of overall function demonstrated <2-fold-decreased affinity for VIIa. The reason for loss of overall function of these mutants requires evaluation on an individual basis in more extensive analyses. One needs to consider that these residues may serve one or several of the following specific functions: (i) Residues may play a role in the assembly and desolvation of the ligand interface, when localized in spatial proximity to key ligand interactive residues. The coagulant assay used for assessment of overall function may be exquisitely sensitive to these on-rate effects. (ii) Similarly, ligand assembly with TF may involve subtle conformational rearrangement which could be perturbed by residue exchange within or in locations distant from the ligand interface. (iii) Specific residues of TF may selectively support

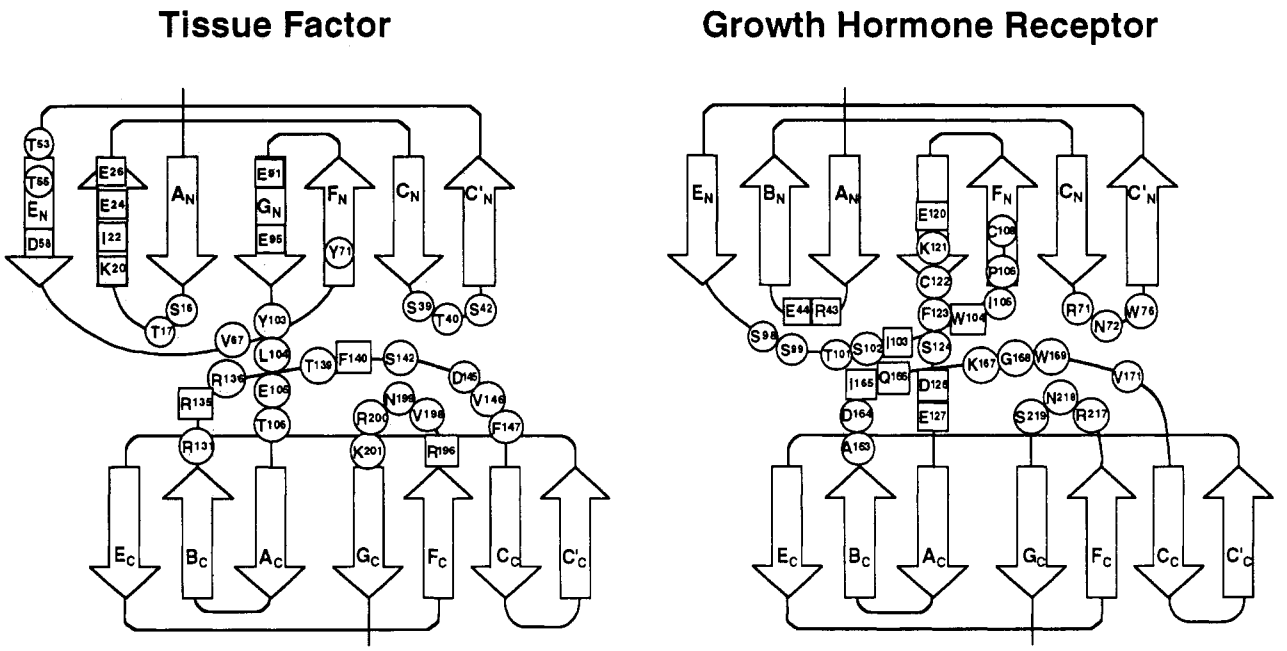

FIGURE 4: Alignment of functional residues in TF with a topology diagram based on the growth hormone receptor structure. Left: Residues with loss of coagulant function (circled) and with >2-fold-increased K_{Dapp} (boxed) are aligned in a topology diagram based on the alignment of the TF sequence (Bazan, 1990) with the growth hormone receptor (De Vos et al., 1992). Some residues are depicted based on the analysis of mutants incorporating multiple residue exchanges, i.e., $Glu^{24} \rightarrow Ala/Glu^{26} \rightarrow Ala$, $Ser^{39} \rightarrow Ala/Thr^{40} \rightarrow Ala/Ser^{42} \rightarrow Ala$, $Thr^{53} \rightarrow Ala/Thr^{55} \rightarrow Ala$, $Glu^{91} \rightarrow Ala/Glu^{95} \rightarrow Ala$. Right: Residues in the growth hormone receptor which form hydrogen bonds or salt bridges with the hormone (boxed) or which have decreased solvent accessibility (circled) in either of the hormone interfaces are displayed in a similar diagram with data taken from the crystallographic solution of the structure of the receptor with growth hormone (De Vos et al., 1992).

the binding of VII and the conversioon to VIIa, and this function would be evaluated in the coagulation assay where VII is present, but not in the K_{Dapp} determination which employed VIIa. (iv) Specific residues in the ligand interface may be selectively required to enhance the catalytic efficiency of the bound VIIa. Single Ala replacement may reduce the catalytic efficiency only slightly, but this reduction in catalytic efficiency could be amplified in the coagulation reaction. Unamplified, as in the K_{Dapp} determination, the slightly decreased catalysis may not have been apparent. (v) There could be interactions of TF unrelated to VII/VIIa binding which influence the overall coagulant function; e.g., certain mutant TF·VIIa complexes may become more susceptible to inactivation by inhibitors present in plasma.

The present analysis identified a limited number of residues which contribute to the binding of VIIa. It is worthwhile to consider that the observed changes in the K_{Dapp}, typically less than 2 orders of magnitude, are frequently observed when single residues are replaced by alanine in protein interactive sites (Bass et al., 1991; Ito et al., 1993; Kelley & O'Connell, 1993). Further, the most significant mutants, $Lys^{20} \rightarrow Ala$, $Ile^{22} \rightarrow Ala$, $Asp^{58} \rightarrow Ala$, $Arg^{135} \rightarrow Ala$, and $Phe^{140} \rightarrow Ala$, could account for more than a 10^6-fold loss of affinity, assuming additivity of the mutational effect, as demonstrated in other studies (Kelley & O'Connell, 1993; Wells, 1990). The seemingly small number of residues which were found to contribute to binding of ligand may thus represent a reasonable percent of the key ligand interface residues. Because the three-dimensional structure of TF has yet to be solved, it is unclear to what extent these residues form a contiguous ligand interface. However, the TF extracellular domain has been predicted (Bazan, 1990; Edgington et al. 1991) to adopt the architectural folding pattern of the cytokine receptor homology domain which consists of a pair of seven-β-strand modules. One can use the predicted alignment of the TF sequence to this type of folding pattern as an initial approach to consider some of the three-dimensional proximity relationships of residues which contribute to function.

The TF sequence is aligned in a topology diagram of two β-strand modules connected by a short sequence from the amino-module strand G_N to the carboxyl-module strand A_C, as shown in Figure 4. This folding topology was found in the structure determination of the growth hormone receptor extracellular domain (De Vos et al., 1992), which is a prototypical cytokine receptor homology domain and predicted to be related to TF (Bazan, 1990). Using this topographical alignment applied to TF, most of the residues which are required for overall function of TF (circled) or VIIa binding (boxed) are in close spatial proximity at the boundary of the two predicted structural modules of the TF extracellular domain. These residues are found predominantly in predicted loops which connect the β-strands. Some of the residues implicated in VIIa binding are also found in putative β-strands, in particular the β-strands B_N and E_N. It is possible that the functional residues clustered at the boundary between the two modules may form a more or less contiguous surface area, which may serve as the ligand interface.

The residues presumed to form the ligand interface in TF are localized in a topographical alignment similar to the ligand interface residues of the growth hormone receptor derived from the crystallographic solution of the growth hormone receptor in complex with its ligand (De Vos et al., 1992). Figure 4 depicts the residues in both structural modules of the receptor which form hydrogen bonds or salt bridges with the hormone (boxed) or which are localized within the desolvated interface (circled). Both growth hormone receptor and TF appear to employ the same loops for contact with their respective ligands. In particular, the loops connecting β-strands A_N–B_N, C_N–C'_N, E_N–F_N, B_C–C_C, or F_C–G_C and the sequence connecting the amino and carboxyl modules appear to be conserved regions for binding of ligand. Despite this overall similarity of the presumed ligand interactive areas,

some differences are apparent. For example, the growth hormone receptor seems to involve more residues in proximity of β-strand F_N and the sequence which connects the two structural modules compared to the findings from mutational analysis of TF. In TF it appears that the β-strands B_N and E_N are important contributors to ligand binding, in contrast to the findings in the growth hormone receptor. It is unclear to what extent these differences result from variations in the actual ligand interface or from uncertainties in the predicted sequence alignment. TF has been assigned to the subclass II of the cytokine receptor family, which includes the interferon receptors, because of structural features distinct from those of the growth hormone receptor and other subclass I cytokine receptors. It is therefore possible that TF and the interferon receptors may adopt a variation of the theme provided by the paradigm of the growth hormone receptor structure and ligand interface.

Other members of the cytokine receptor family may also employ the same regions for ligand recognition. This can be demonstrated at some key residue positions from emerging mutational analyses of members of this receptor family. In the B_C–C_C loop at the position of Arg^{135} and Arg^{136} in TF, contact residues have been identified not only in the growth hormone receptor (Ile^{165}, Gln^{166}) but also in two other cytokine receptors, the interleukin-2 receptor β-chain (Imler et al., 1992) and the murine interleukin-3 receptor (Wang et al., 1992). The prolactin receptor, which is closely related to the growth hormone receptor, employs the A_N–B_N loop for binding ligand (Rozakis-Adcock & Kelly, 1992). This is also found for TF and the growth hormone receptor. Extensive mutational analysis of the interleukin-6 receptor further provided data consistent with an assignment of the ligand interface at the boundary of the two predicted structural modules (Yawata et al., 1993). This comparison of the ligand interactive area in TF with other cytokine receptors thus suggests that ligand recognition by the two structural modules is architecturally conserved throughout the receptor family. Indeed, molecular recognition through a tandem pair of structural modules may be more widely used in protein–protein interactions, as demonstrated by the suggested involvement of at least two adjacent type III repeats in fibronectin for interaction with integrins (Main et al., 1992; Kimizuka et al., 1991; Bowditch et al., 1991) or by antigen recognition in the immunoglobulin family (Hunkapiller & Hood, 1989). Similar to immunoglobulin modules, the cytokine receptors appear to employ several surface loops to create structure with specificity for recognition of ligand. In immunoglobulins, the paired recognition of ligand is achieved by parallel alignment of light and heavy chains; thus loops at the same pole in both modules are used for binding of ligand. In contrast, the cytokine receptor family employs tandem alignment of a similar structural framework. This results in recognition of ligand at the boundary between modules which contribute surface loops from opposite poles. Diversity in recognition of ligands may be generated by variability in the primary sequence and in the length of loops which form the ligand interface. In addition, the architecture of the recognition site can be predicted to depend on the relative orientation of the two structural modules at the intermodule boundary.

The ligand binding site of cytokine receptors appears to recognize helical ligands. Although very short helical stretches may be associated with the predominant β-structure of epidermal growth factor-like (EGF) domains (Hommel et al. 1992), recognition of a paired helical motif appears to be replaced by recognition of two EGF modules of VIIa in the example of TF (Toomey et al., 1991). However, further complexity is introduced by the proposed contribution of protease domain residues in VIIa to the interaction with TF (O'Brien et al., 1991; Kazama et al., 1993) and a potential role of the γ-carboxyglutamic acid rich domain in factor VII in TF interaction (Sakai et al., 1990; Ruf et al., 1991a). The complementary binding site in VIIa may thus be formed by residues in different structural modules which associate to form a contiguous interactive structure. Although built from protein modules with structural scaffolds different from the helical cytokines, the interactive site in VIIa could potentially share some of the structural characteristics of the receptor interface of cytokine ligands. The structural elucidation of the TF–VIIa interface and the comparison with ligand interfaces of other members of the cytokine receptor family promise to provide more general rules for how the structural scaffold of two β-strand modules allows both diversity and specificity of ligand recognition.

ACKNOWLEDGMENT

We thank Dr. Peter E. Wright for discussion of the NMR data, Pablito Tejada, David Revak, and Cindi Biazak for technical assistance, and Barbara Parker for preparation of the manuscript.

REFERENCES

Bass, S. H., Mulkerrin, M. G., & Wells, J. A. (1991) *Proc. Natl. Acad. Sci. U.S.A. 88*, 4498.
Bazan, J. F. (1990) *Proc. Natl. Acad. Sci. U.S.A. 87*, 6934.
Bowditch, R. D., Halloran, C. E., Aota, S.-I., Obara, M., Plow, E. F., Yamada, K. M., & Ginsberg, M. H. (1991) *J. Biol. Chem. 266*, 23323.
Davie, E. W., Fujikawa, K., & Kisiel, W. (1991) *Biochemistry 30*, 10363.
De Vos, A. M., Ultsch, M., & Kossiakoff, A. A. (1992) *Science 255*, 306.
Edgington, T. S., Mackman, N., Brand, K., & Ruf, W. (1991) *Thromb. Haemostasis 66*, 67.
Hommel, U., Harvey, T. S., Driscoll, P. C., & Campbell, I. D. (1992) *J. Mol. Biol. 227*, 271.
Hunkapiller, T., & Hood, L. (1989) *Adv. Immunol. 44*, 1.
Imler, J.-L., Miyajima, A., & Zurawski, G. (1992) *EMBO J. 11*, 2047.
Ito, W., Iba, Y., & Kurosawa, Y. (1993) *J. Biol. Chem. 268*, 16639.
Jones, D. H., & Howard, B. H. (1991) *BioTechniques 10*, 62.
Kazama, Y., Pastuszyn, A., Wildgoose, P., Hamamoto, T., & Kisiel, W. (1993) *J. Biol. Chem. 268*, 16231.
Kelley, R. F., & O'Connell, M. P. (1993) *Biochemistry 32*, 6828.
Kimizuka, F., Ohdate, Y., Kawase, Y., Shimojo, T., Taguchi, Y., Hashino, K., Goto, S., Hashi, H., Kato, I., Sekiguchi, K., & Titani, K. (1991) *J. Biol. Chem. 266*, 3045.
Krishnaswamy, S. (1992) *J. Biol. Chem. 267*, 23696.
Lawson, J. H., Butenas, S., & Mann, K. G. (1992) *J. Biol. Chem. 267*, 4834.
Main, A. L., Harvey, T. S., Baron, M., Boyd, J., & Campbell, I. D. (1992) *Cell 71*, 671.
Miyajima, A., Bond, M. W., Otsu, K., Arai, K.-I., & Arai, N. (1985) *Gene 37*, 155.
Nakagaki, T., Foster, D. C., Berkner, K. L., & Kisiel, W. (1991) *Biochemistry 30*, 10819.
O'Brien, D. P., Gale, K. M., Anderson, J. S., McVey, J. H., Miller, G. J., Meade, T. W., & Tuddenham, E. G. D. (1991) *Blood 78*, 132.
O'Brien, D. P., Anderson, J. S., Martin, D. M. A., Byfield, P. G. H., & Tuddenham, E. G. D. (1993) *Biochem. J. 292*, 7.
Ösapay, K., & Case, D. A. (1991) *J. Am. Chem. Soc. 113*, 9436.

Rao, L. V. M., & Rapaport, S. I. (1988) *Proc. Natl. Acad. Sci. U.S.A. 85*, 6687.
Rehemtulla, A., Ruf, W., & Edgington, T. S. (1991) *J. Biol. Chem. 266*, 10294.
Roy, S., Hass, P. E., Bourell, J. H., Henzel, W. J., & Vehar, G. A. (1991) *J. Biol. Chem. 266*, 22063.
Rozakis-Adcock, M., & Kelly, P. A. (1992) *J. Biol. Chem. 267*, 7428.
Ruf, W., & Edgington, T. S. (1991a) *Thromb. Haemostasis 66*, 529.
Ruf, W., & Edgington, T. S. (1991b) *Proc. Natl. Acad. Sci. U.S.A. 88*, 8430.
Ruf, W., Kalnik, M. W., Lund-Hansen, T., & Edgington, T. S. (1991a) *J. Biol. Chem. 266*, 15719.
Ruf, W., Rehemtulla, A., & Edgington, T. S. (1991b) *Biochem. J. 278*, 729.
Ruf, W., Rehemtulla, A., Morrissey, J. H., & Edgington, T. S. (1991c) *J. Biol. Chem. 266*, 2158.
Ruf, W., Miles, D. J., Rehemtulla, A., & Edgington, T. S. (1992a) *J. Biol. Chem. 267*, 22206.
Ruf, W., Miles, D. J., Rehemtulla, A., & Edgington, T. S. (1992b) *J. Biol. Chem. 267*, 6375.
Ruf, W., Stura, E. A., LaPolla, R. J., Syed, R., Edgington, T. S., & Wilson, I. A. (1992c) *J. Cryst. Growth 122*, 253.
Ruf, W., Miles, D. J., Rehemtulla, A., & Edgington, T. S. (1993) *Methods Enzymol. 222*, 209.
Sakai, T., Lund-Hansen, T., Thim, L., & Kisiel, W. (1990) *J. Biol. Chem. 265*, 1890.
Toomey, J. R., Smith, K. J., & Stafford, D. W. (1991) *J. Biol. Chem. 266*, 19198.
Wang, H.-M., Ogorochi, T., Arai, K., & Miyajima, A. (1992) *J. Biol. Chem. 267*, 979.
Waxman, E., Ross, J. B. A., Laue, T. M., Guha, A., Thiruvikraman, S. V., Lin, T. C., Konigsberg, W. H., & Nemerson, Y. (1992) *Biochemistry 31*, 3998.
Wells, J. A. (1990) *Biochemistry 29*, 8509.
Yawata, H., Yasukawa, K., Natsuka, S., Murakami, M., Yamasaki, K., Hibi, M., Taga, T., & Kishimoto, T. (1993) *EMBO J. 12*, 1705.